

Cures from the ocean: Marine organisms synthesize complex metabolites with antibacterial properties (see picture) to fend off co-occurring microbes. Representatives from each of five classes of natural products (ribosomal and non-ribosomal peptides, polyketides, alkaloids, and terpenes) isolated as new antibacterial metabolites from marine organisms are described (picture courtesy of X. Alvarez-Micó).



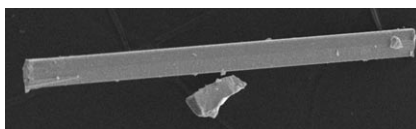
Natural Products

C. C. Hughes,
W. Fenical* 12512–12525

Antibacterials from the Sea

CORRESPONDENCE

From nanorods to micropisms: The crystal structure of recently reported Ba₇F₁₂Cl₂ nanorods is shown to correspond to the structure of Ba₇F₁₂Cl₂ (see picture), which can be prepared by several growth techniques.

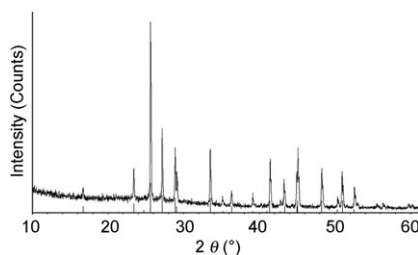


Nanorods

F. Kubel,*
H.-R. Hagemann 12526–12527

Comment on: “Nucleation and Growth of BaF_xCl_{2-x} Nanorods”

Taken in good faith: The structure of the nanorods indexed as “Ba₂F₃Cl” was based on the similarity of the X-ray diffraction pattern with that given on the JCPDS card (No. 07-0029) for the above-mentioned structure. It appears, however, that the structure should have been indexed as “Ba₇F₁₂Cl₂” in line with more recent results.



Nanorods

M. Gong, T. Xie, Y. Li* 12528

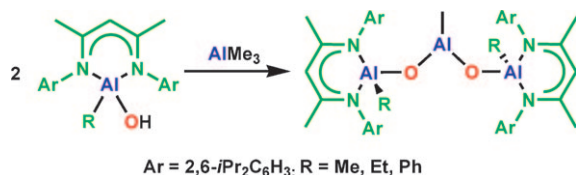
Reply to Comment on: “Nucleation and Growth of BaF_xCl_{2-x} Nanorods”

COMMUNICATIONS

Alumoxanes

Y. Yang, H. Zhu, H. W. Roesky,*
Z. Yang, G. Tan, H. Li,* M. John,
R. Herbst-Irmer 12530–12533

Trinuclear Alumoxanes with an Acyclic Al-O-Al-O-Al Core and Studies of Their Reactivity



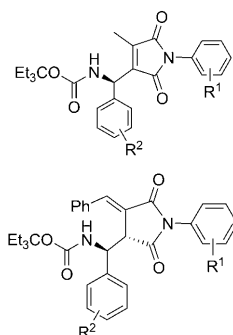
No cycle this time: The first trinuclear alumoxanes [(LAlR(μ-O))₂AlMe] (L = CH[C(Me)N(Ar)]₂; Ar = 2,6-*i*Pr₂C₆H₃; R = Me, Et, Ph) with an acyclic Al-O-Al-O-Al core were synthesized (see scheme). The ethyl and

phenyl derivatives were characterized by X-ray spectroscopy. When treated with AlMe₃, [(LAlR(μ-O))₂AlMe] (R = Me, Ph) gave tetranuclear alumoxanes bearing a (Me₂AlO)₂ four-membered ring.

Asymmetric Synthesis

J. Wang, H. Liu, Y. Fan, Y. Yang,
Z. Jiang,* C.-H. Tan* 12534–12537

Bicyclic Guanidine-Catalyzed Direct Asymmetric Allylic Addition of *N*-Aryl Alkylidene-Succinimides

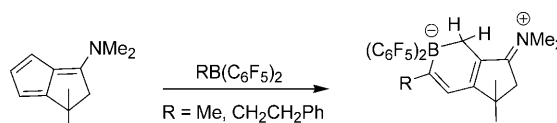


Enantio-enriched maleimides and succinimides that can be used to prepare aza-heterocycles with multiple chiral centers are obtained from the bicyclic guanidine-catalyzed direct asymmetric allylic addition of *N*-aryl alkylidene-succinimides to imines. NMR studies and deuterium-exchange experiments were used to study the intermediates in the reaction.

C–C Activation

B.-H. Xu, G. Kehr, R. Fröhlich,
G. Erker* 12538–12540

Carbon–Carbon Bond Cleavage by Strongly Electrophilic Boranes



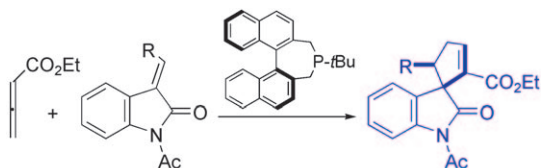
Make and break: Strongly electrophilic boranes $RB(C_6F_5)_2$ ($R = Me, CH_2CH_2Ph$) react with an aminodihydropentalene substrate by C=C bond

cleavage with concomitant borylene insertion to yield the ring-enlarged zwitterionic borate/iminium product.

Organocatalysis

A. Voituriez, N. Pinto, M. Neel,
P. Retailleau,
A. Marinetti* 12541–12544

An Organocatalytic [3+2] Cyclisation Strategy for the Highly Enantioselective Synthesis of Spirooxindoles



17 examples, ee = 94 to >99%

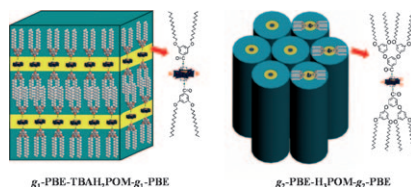
Power of P: Phosphine-promoted [3+2] annulation reactions between electron-poor allenes and 3-arylidene indolin-2-ones afford a new organocatalytic strategy for the synthesis of the spirocyclic core of oxindolic cyclopentanes (see scheme). Asymmetric variants of these reactions have been implemented by using chiral catalysts, giving very high levels of asymmetric induction.

Asymmetric variants of these reactions have been implemented by using chiral catalysts, giving very high levels of asymmetric induction.

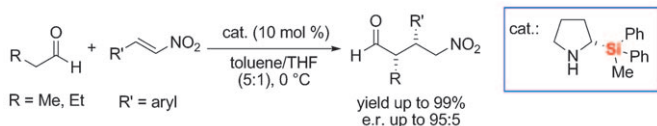
Dendron–Polyoxometalate Hybrids

Y. L. Wang, X. L. Wang, X. J. Zhang,
N. Xia, B. Liu, J. Yang, W. Yu,
M. B. Hu, M. Yang,
W. Wang* 12545–12548

Manipulation of Ordered Nanostructures of Protonated Polyoxometalate through Covalently Bonded Modification



Let there be order: By covalently grafting first- and second-generation dendrons to a polyoxometalate (POM), lamellar or cylindrical nanostructures of the protonated dendron-POM-dendron hybrids have been constructed (see figure), which may open an avenue to the future fabrication of novel solid proton conductors with highly ordered structures.



Silicon can! A convenient synthesis of enantiopure (*S*)-2-(diphenylmethylsilyl)pyrrolidine is described and its organocatalytic activity in asymmetric Michael reactions is demonstrated (see scheme). By using 10 mol % of this

novel organocatalyst, the addition of aldehydes to nitroolefins affords products with high stereoselectivities (d.r. $\leq 97:3$ and e.r. $\leq 95:5$) in yields up to 99 %.

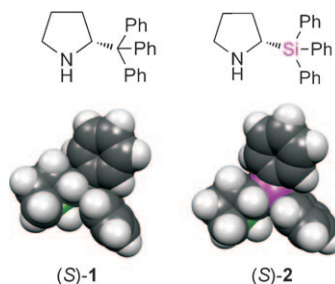
Silicon Organocatalysis

*R. Husmann, M. Jörres, G. Raabe, C. Bolm** 12549–12552

Silylated Pyrrolidines as Catalysts for Asymmetric Michael Additions of Aldehydes to Nitroolefins



Silicon-based organocatalysts: In an effort to study the effects of substituting carbon by silicon within the catalyst backbone, we developed an efficient synthesis of (*S*)-2-triphenylsilylpyrrolidine [(*S*)-**2**]. The evaluation of (*S*)-**2** against its carbon analogue (*S*)-**1** in two organocatalytic reactions is complemented by computational studies.



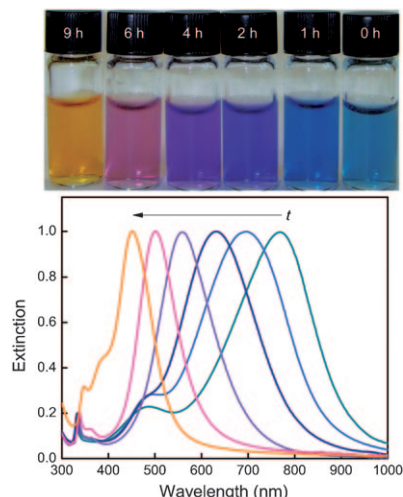
Silicon Organocatalysis

J. O. Bauer, J. Stiller, E. Marqués-López, K. Strohfeldt, M. Christmann, C. Strohmann** 12553–12558

Silyl-Modified Analogues of 2-Triptylpyrrolidine: Synthesis and Applications in Asymmetric Organocatalysis



Sharp change indicators: A new class of time–temperature indicators (TTIs) based upon aqueous suspensions of triangular silver nanoplates with relatively sharp corners has been developed. Such nanoplates display localized surface plasmon resonance peaks in the visible region, the positions of which are highly sensitive to the sharpness of the corners.



Sensors

*J. Zeng, S. Roberts, Y. Xia** 12559–12563

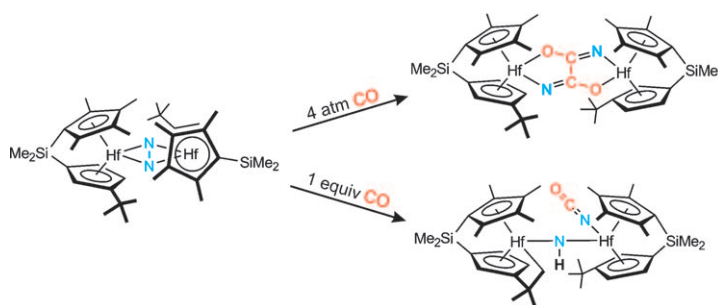
Nanocrystal-Based Time–Temperature Indicators



Nitrogen Fixation

X. Zhang, B. Butschke,
H. Schwarz* 12564–12569

**N₂ Activation by a Hafnium Complex:
A DFT Study on CO-Assisted
Dinitrogen Cleavage and
Functionalization**



Let's break it completely: Activation and functionalization of dinitrogen constitute challenging goals. Chirik and co-workers have studied the reaction of a hafnocene–dinitrogen complex with CO in the course of which the N–N bond is completely broken. Computational studies on mechanistic

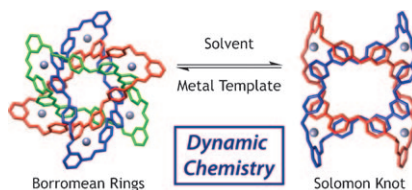
features of this particular reaction show that migratory insertion of CO into the Hf–N bond, that is, C–N bond formation, is easy and that the release of ring strain of a four-membered Hf–C–N–N ring provides the driving force for N–N bond scission.

FULL PAPERS

Self-Assembly

C. D. Meyer, R. S. Forgan,
K. S. Chichak, A. J. Peters,
N. Tangchaivang, G. W. V. Cave,
S. I. Khan, S. J. Cantrill,
J. F. Stoddart* 12570–12581

**The Dynamic Chemistry of Molecular
Borromean Rings and Solomon Knots**

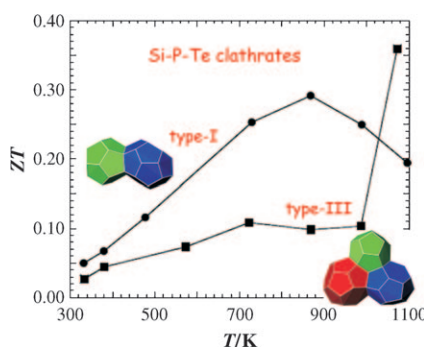


One thing one minute and another the next: The dynamic solution equilibria between molecular Borromean rings and Solomon knots (see figure) are examined with respect to synthetic conditions, choice of metal template, and crystallization protocols in the self-assembly of these topologically complex mechanically interlocked architectures.

Clathrates

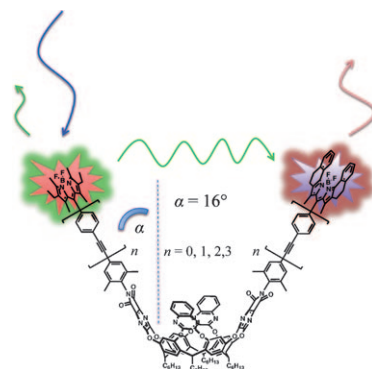
J. V. Zaikina, T. Mori, K. Kovnir,
D. Teschner, A. Senyshyn, U. Schwarz,
Yu. Grin,
A. V. Shevelkov* 12582–12589

**Bulk and Surface Structure and High-
Temperature Thermoelectric Properties
of Inverse Clathrate-III in the
Si-P-Te System**



Thermoelectric Si-P-Te clathrate-III: Si-P-Te clathrate-III has been developed as a new high-temperature thermoelectric material. Its utmost stability (up to 1500 K) in air is the result of the formation of a nanosized surface layer of phosphorus-doped silica. The as-prepared Si-P-Te clathrate displays high values of the thermoelectric figure-of-merit at temperatures up to 1100 K (see figure). Further methods of thermoelectric efficiency optimization for Si-P-Te clathrates are discussed.

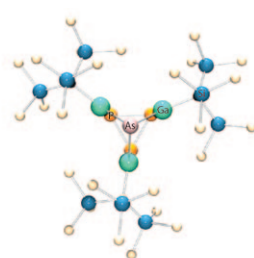
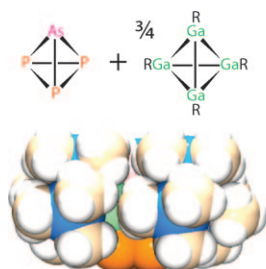
Shed light on it! A series of BODIPY-dye-labeled resorcin[4]arene cavitands with oligo(phenylene-ethynylene) spacers of different lengths were synthesized; their pH- and temperature-dependent switching behavior was studied. Distance parameters from X-ray structures of synthetic intermediates combined with results from fluorescence resonance energy transfer (FRET) studies enabled the determination of the average opening angle (α) of the cavitands in the vase conformation in solution (see scheme).



Cavitands

*I. Pochorovski, B. Breiten,
W. B. Schweizer,
F. Diederich** 12590–12602

FRET Studies on a Series of BODIPY-Dye-Labeled Switchable Resorcin[4]arene Cavitands



Cluster Compounds

*B. M. Cossairt,
C. C. Cummins** 12603–12608

Molecular Gallium Arsenide Phosphide Clusters Prepared from AsP_3 , P_4 , and $[\{\text{GaC}(\text{SiMe}_3)_3\}_4]$

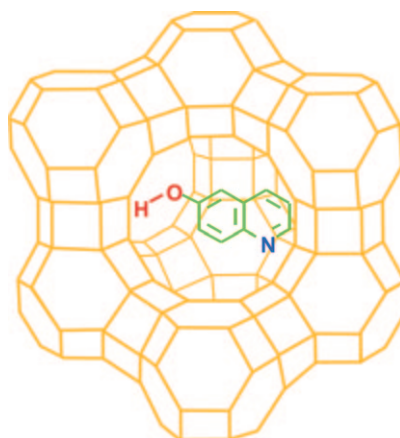


When tetrahedra collide: The reaction of AsP_3 with $[\{\text{GaC}(\text{SiMe}_3)_3\}_4]$ provides access to molecular gallium arsenide phosphide clusters. In particular, $[\text{As}\{\text{GaC}(\text{SiMe}_3)_3\}_3\text{P}_3]$ was prepared, in

which three $\{\text{GaC}(\text{SiMe}_3)_3\}$ units have inserted into all three AsP bonds of AsP_3 , with a lone Ga-supported As atom and an intact *cyclo*- P_3 ring (see graphic).

Equilibrium dynamics in zeolites:

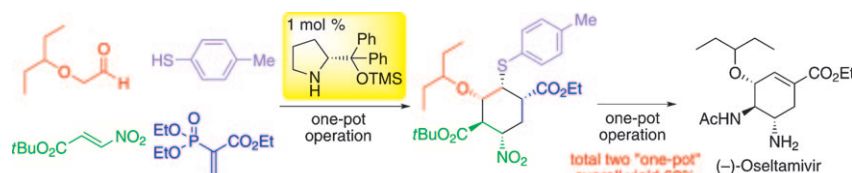
Excited-state proton transfer and geminate recombination of 6-hydroxyquinoline encaged in faujasite zeolites (see picture) have been investigated. Proton transfer at each tautomerization step of 6-hydroxyquinoline is in competition with geminate recombination due to the confined environment of dehydrated zeolitic supercages. Thus, excited-state equilibria among three prototropic species of 6-hydroxyquinoline are established.



Host-Guest Systems

*S.-Y. Park, H. Yu, J. Park,
D.-J. Jang** 12609–12615

Excited-State Prototropic Equilibrium Dynamics of 6-Hydroxyquinoline Encapsulated in Microporous Catalytic Faujasite Zeolites



Fighting the flu: Two “one-pot” and column-free asymmetric sequences are used to accomplish the synthesis of (–)-oseltamivir, known as the anti-influenza drug Tamiflu (see scheme;

TMS: trimethylsilyl). This high-yielding synthesis takes advantage of a diphenylprolinol silyl ether as an organocatalyst and single-pot domino operations.

Asymmetric Synthesis

*H. Ishikawa, T. Suzuki, H. Orita,
T. Uchimaru,
Y. Hayashi** 12616–12626

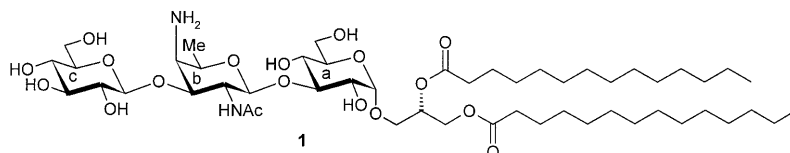
High-Yielding Synthesis of the Anti-Influenza Neuraminidase Inhibitor (–)-Oseltamivir by Two “One-Pot” Sequences



Oligosaccharides

C. M. Pedersen, I. Figueroa-Perez,
J. Boruwa, B. Lindner, A. J. Ulmer,
U. Zähringer,
R. R. Schmidt* 12627–12641

Synthesis of the Core Structure of the Lipoteichoic Acid of *Streptococcus pneumoniae*



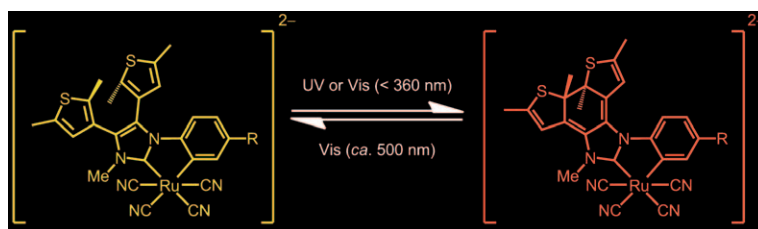
The core: The synthesized core structure (1) of *S. pneumoniae* LTA (lipoteichoic acid) exhibited similar stimulation of interleukin-8 release as the recently synthesized complete LTA

consisting of the core structure and the pseudopentasaccharidic repeating unit. Contrary to previous postulations, TLR2 is not the signalling receptor for these compounds.

Photochromism

G. Duan, V. W.-W. Yam* 12642–12649

Syntheses and Photophysical Properties of *N*-Pyridylimidazol-2-ylidene Tetracyanoruthenates(II) and Photochromic Studies of Their Dithienylethene-Containing Derivatives



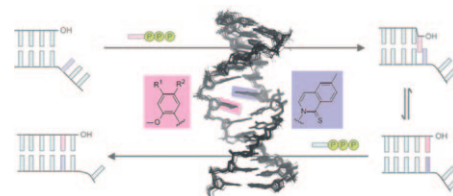
Enlightening chemistry: Luminescent tetracyanoruthenates(II) with chelating pyridyl *N*-heterocyclic carbene ligands have been synthesized and their dithi-

enylethene-containing complexes have been shown to display interesting photochromic properties (see figure).

Unnatural Base Pairs

D. A. Malyshev, D. A. Pfaff,
S. I. Ippoliti, G. T. Hwang,
T. J. Dwyer,*
F. E. Romesberg* 12650–12659

Solution Structure, Mechanism of Replication, and Optimization of an Unnatural Base Pair



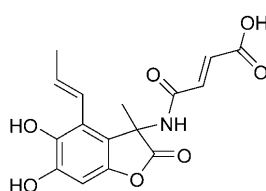
Optimization of the unnatural: A variety of derivatized unnatural base pairs have been synthesized and their structures and DNA polymerase-mediated replication have been evaluated (see

graphic). The data elucidate the mechanism of replication and one pair, dDMO-d5SICS, represents significant progress towards the expansion of the genetic alphabet.

Natural Products

P. J. Gross, S. Bräse* 12660–12667

The Total Synthesis of (±)-Fumimycin



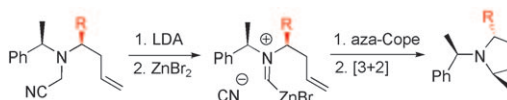
fumimycin

Peptide deformylase (PDF)-inhibitor synthesis: A strategy involving amine formation through addition to a ketimine has been successfully employed for the first total synthesis of the antibiotic agent fumimycin (see scheme).

Cyclization

S. Ouizem, S. Cheramy, C. Botuha,
F. Chemla,* F. Ferreira,
A. Pérez-Luna 12668–12677

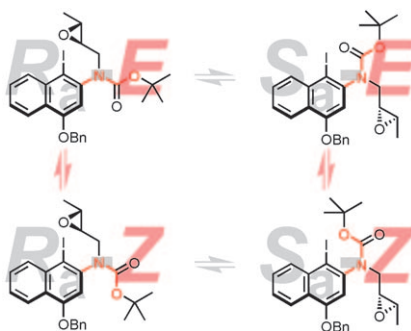
Cyclization of Zincated α -*N*-Homallylamino Nitriles: A New Entry to Enantiopure 2,3-Methanopyrrolidines



Cyclizing with zinc: Zincated α -*N*-homallylamino nitriles lead to 2,3-methanopyrrolidines in good yields and excellent selectivities (see scheme; LDA = lithium diisopropylamide). The cyclization occurs with a stereospecific inver-

sion of the homoallylic stereogenic center, which has been rationalized by a mechanism involving the formation of a zincioiminium ion that undergoes an aza-Cope rearrangement followed by [3+2] cycloaddition.

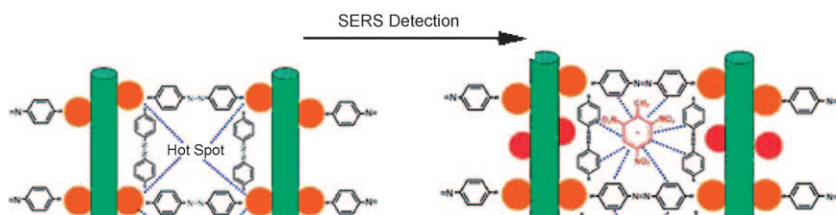
In a tight spot: The depicted *N*-aryl-*N*-alkylcarbamate (Bn = benzyl) exists as four atropo-diastereomers at room temperature due to hindered rotation about the *N*-aryl and *N*-C(O) bonds. By using 2D exchange NMR spectroscopy (EXSY), the height of the rotational barriers could be determined and compared to those of three related compounds.



Carbamates

L. F. Tietze, H. J. Schuster, J. M. von Hof, S. M. Hampel, J. F. Colunga, M. John** ... 12678–12682

Atropisomerism of Aromatic Carbamates



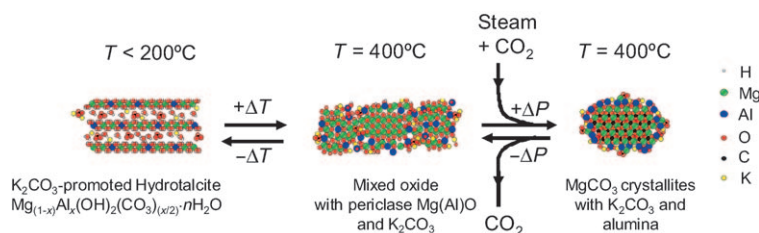
SERS substrates: The ultra-trace detection of TNT based on surface-enhanced Raman scattering (SERS) is reported. The method relies on π -donor–acceptor interactions between the π -acceptor TNT and the π -donor

p,p'-dimercaptoazobenzene (DMAB), with the latter serving to cross-link silver nanoparticles deposited on the surface of silver molybdate nanowires (see scheme).

TNT Detection

L. Yang, L. Ma, G. Chen, J. Liu, Z.-Q. Tian* 12683–12693

Ultrasensitive SERS Detection of TNT by Imprinting Molecular Recognition Using a New Type of Stable Substrate



CO₂ sponge cleans up! K₂CO₃-promoted hydrotalcite shows outstanding CO₂ storage capacity at relatively high temperature and pressure. In situ structural studies demonstrate that

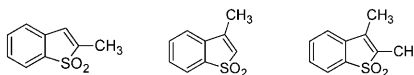
magnesium oxide centres of the hydrotalcite-based materials are converted to magnesium carbonate above 300 °C under sufficient CO₂ and steam pressure (see picture).

Carbon Dioxide Storage

S. Walspurger, P. D. Cobden, O. V. Safonova, Y. Wu, E. J. Anthony* 12694–12700

High CO₂ Storage Capacity in Alkali-Promoted Hydrotalcite-Based Material: In Situ Detection of Reversible Formation of Magnesium Carbonate

Discovering the unknown: This computational study explores the relationship between the molecular structure and the solid-state structure for three small molecules (see scheme) that are known to crystallise in distinct crystal structures. By using accurate lattice-energy calculation tools, it is predicted that another, as yet undiscovered, polymorph should exist for the dimethyl-substituted compound.



Crystal Structures

*A. Asmadi, J. Kendrick, F. J. J. Leusen** 12701–12709

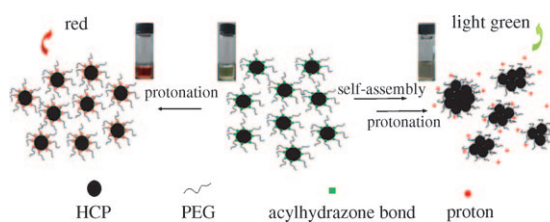
Crystal Structure Prediction and Isostructurality of Three Small Molecules



Conjugated Polymers

F. Qiu, C. Tu, Y. Chen, Y. Shi, L. Song, R. Wang, X. Zhu,* B. Zhu,* D. Yan, T. Han* 12710–12717

Control of the Optical Properties of a Star Copolymer with a Hyperbranched Conjugated Polymer Core and Poly(ethylene glycol) Arms by Self-Assembly



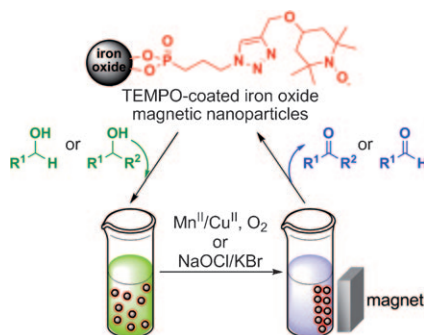
Tuning a star copolymer: A star copolymer (HCP-*star*-PEG) with a hyperbranched conjugated (HCP) core and many poly(ethylene glycol) (PEG) arms has been synthesized through an acylhydrazone connection. The optical properties of HCP-*star*-PEG changed

on complexation of acid (see figure). With different proportions of chloroform and acetonitrile, the optical properties of HCP-*star*-PEG can be easily controlled by self-assembly of the star polymer.

Heterogeneous Catalysis

A. K. Tucker-Schwartz, R. L. Garrell* 12718–12726

Simple Preparation and Application of TEMPO-Coated Fe₃O₄ Superparamagnetic Nanoparticles for Selective Oxidation of Alcohols

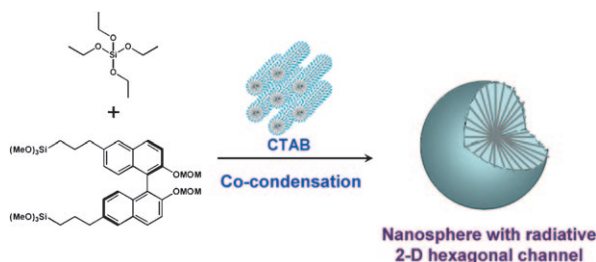


Recycling to a different TEMPO: An extremely simple and economic synthesis of a recyclable 2,2,4,4-tetramethylpiperidine-1-oxyl (TEMPO)-coated superparamagnetic catalyst is described. The catalyst shows excellent performance in the rapid oxidation of primary and secondary benzylic and aliphatic alcohols by using oxygen and Mn^{II}/Cu^{II} or biphasic NaOCl/KBr conditions.

Mesoporous Materials

X. Liu, P. Wang, L. Zhang, J. Yang, C. Li,* Q. Yang* 12727–12735

Chiral Mesoporous Organosilica Nanospheres: Effect of Pore Structure on the Performance in Asymmetric Catalysis



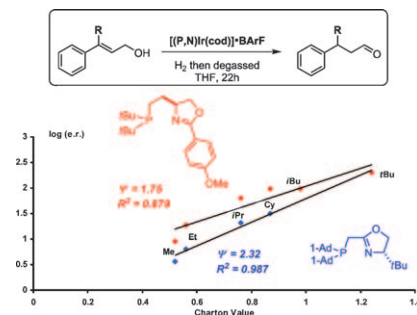
Spheres of influence: (*R*)-(+)-Binol-functionalized chiral periodic mesoporous organosilicas (PMOs) with different pore structures and morphology are efficient catalysts for the asymmetric addition of diethylzinc to aldehydes. Nanospheres with a radiative

2D hexagonal channel arrangement show the highest activity and *ee* value of the chiral PMOs investigated (see picture; MOM: methoxymethyl ether, CTAB: cetyltrimethylammonium bromide).

Asymmetric Catalysis

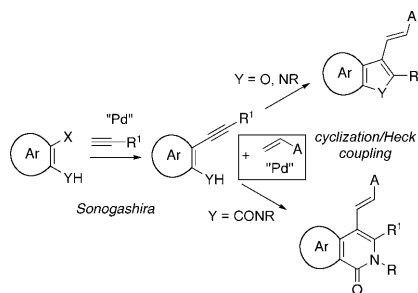
L. Mantilli, D. Gérard, S. Torche, C. Besnard, C. Mazet* ... 12736–12745

Improved Catalysts for the Iridium-Catalyzed Asymmetric Isomerization of Primary Allylic Alcohols Based on Charton Analysis



Achieving enantioselectivity: An improved generation of chiral cationic iridium catalysts for the asymmetric isomerization of primary allylic alcohols is disclosed. The design of these air-stable complexes relies on preliminary mechanistic information and on Charton analyses using two preceding generations of iridium catalysts developed for this highly challenging transformation (see figure).

Cascade synthesis: Benzofuran-, indole-, and isoquinolone-type derivatives are prepared using consecutive Sonogashira and cascade Pd-catalyzed heterocyclization/oxidative Heck couplings from readily available 2-halo-substituted phenol, aniline, and benzamide substrates, alkynes and functionalized olefins (see scheme).





Heterocycle Synthesis


R. Álvarez, C. Martínez, Y. Madich, J. G. Denis, J. M. Aurrecoechea,* Á. R. de Lera** 12746–12753

A General Synthesis of Alkenyl-Substituted Benzofurans, Indoles, and Isoquinolones by Cascade Palladium-Catalyzed Heterocyclization/Oxidative Heck Coupling

* Author to whom correspondence should be addressed

 Supporting information on the WWW (see article for access details).

 Full Papers labeled with this symbol have been judged by two referees as being “very important papers”.

 A video clip is available as Supporting Information on the WWW (see article for access details).

SERVICE

Spotlights _____ 12506 Author Index _____ 12756 Keyword Index _____ 12757 Preview _____ 12759

Issue 41/2010 was published online on October 26, 2010



Fast, Individual, Popular...
REPRINTS
Available to order anytime!
 Contact Carmen Leitner (e-mail: chem-reprints@wiley.com)